Structural Health Monitoring of Glass Fiber Reinforced Polymer Using Nanofiber Sensor

M. S. Nisha, P. Faruk Khan and K. V. Ravali

Abstract Nowadays, GFRP, i.e., glass fiber reinforced polymer composites, are widely used in manufacturing process especially in aircraft industries and automobiles due to their beneficial mechanical and thermal properties such as specific strength and better resistance to corrosion. In this present research, the electrostatic-bonded PVDF-MWCNT fiber composition and GFRP had been used for structural health monitoring (SHM) of composite material. PVDF-MWCNT had been embedded to upper-most layer of the nonconductive materials which is GFRP, i.e., glass fiber reinforced polymers for the undertaking process. This research takes place mainly to improve the multifunction ability. Mainly, the manufacture specimen was characterized into two types; they are mechanical load characterization and material characterization. It is the first time this fiber composition is used in composite materials for monitoring purposes. MWCNT fiber easily penetrates and does not decrease the mechanical properties of material. In this investigation, SEM, i.e., scanning electron microscope and XRD (X-ray diffraction) were used for material characterization process to determine the dispersion of MWCNT with polymer, crystalline structure. The manufactured specimen another characterization namely mechanical load characterization it had done in two ways are incremental–decremental tensile loading and three-point loading testing in order to determine the sensitivity of the material during loading and unloading, material damage identification. The MWCNT fiber worked as a sensor in both tensile and compression loadings. So we mainly used the MWCNT for this process.

Keywords GFRP · SEM · XRD · PVDF-MWCNT · Electrical resistance SHM

M. S. Nisha (✉) · P. Faruk Khan · K. V. Ravali
School of Aeronautical Sciences, Hindustan Institute of Technology and Science, Chennai 603103, India
e-mail: msnisha@hindustanuniv.ac.in

K. S. Vijay Sekar et al. (eds.), *Advances in Manufacturing Processes*, Lecture Notes in Mechanical Engineering, https://doi.org/10.1007/978-981-13-1724-8_24

1 Introduction

In the present aviation and aerospace industries, composites are vigorously employing due to their esteemed properties such as low structural weight, high stiffness, corrosion resistance, higher resistance to defect or damage and thermal, physical properties which reduce the current uncertainties in the aviation terrain [1]. Nowadays, composites are used in different applications for lightweight, strength and have improved structural performance [2], so that glass fiber reinforced polymer (GFRP) will be used in aircraft structures like in landing gears, engine parts, fuselage and wings [3] due to its high strength-to-weight ratio, low maintenance cost, excellent corrosion resistant, high specific strength, high specific and good resistant to chemical agents [4]. At present, the failure of an aircraft is due to structural deterioration and the most probably failure in an aircraft is fatigue damage, buckling, scratches, notches, etc. The fatigue damage is caused due to the high stress concentration point when a load is applied in localized zone [5] and the buckling also leads the failure of aircraft, reducing the bending stiffness and shear stiffness [6]. There are many techniques which were adopted to identify the damages on the aircraft structures [7], such as visual inspection, ultrasonic testing, thermography and tomography. All these damage sensing methods were adopted for the composite structures where the sensors were embedded between the structures. And all techniques have its own advantages and disadvantages based on their applications, such as visual inspection can only detect the surface cracks and damages. It will be useful to identify the flaws on the surface but not underneath the surface. In general, visual inspection practice depends heavily on the vision (or) experience of the inspector [8]. Embedding ultrasonic sensor, piezoelectric sensor and acoustic emission in the literature to detect the damages on the aircraft structures [9–11]. This technique has two units in which one unit generates the wave field and other unit receives the signal. These generated waves penetrate the composite structure if there is any damage which delays propagation of signals. However, they have some drawbacks: embedding sensor downgrades the mechanical property of the specimen [12]. Meanwhile, during the manufacturing process, the embedding sensor itself gets damage due to the high pressure and temperature applied to the sensor. And even in the optical fiber sensor, the signal ion may be found when the damage has realized on the structure. The detection of this damage by using the above-mentioned techniques is known as structural health monitoring (SHM). SHM illustrates the system that can monitor the virtue of a design [13]. It is programmed condition computation of the design through examination and analysis of the data collected on-site by sensing system. This approach will determine the location of damage by using sensors which are sensitive to changes in single parameter and in sensitive to change other parameters [14]. The aircraft SHM system appears in landing gear monitoring, engines and composite structures. While most of the aircraft structures other than composite structures are made from ductile alloys that can endure crack growth over time, brittle alloys have high strength where these differences will effect the SHM [15].

The nanotechnology plays a vital role in SHM where the material itself acts as the sensor so that it will not degrade the mechanical property of aircraft structures. The implementation of carbon nanotubes in the sensor technology (SHM) of the aircraft composite structures by embedding the PVDF and MWCNT in the GFRP to detect the damages in the aircraft composites. As a nanotube is a surface structure, its whole weight is concentrated in the surface of its layers. The extremely high adsorption capacity of the MWCNT and the excellent sensitivity of the MWCNT properties to atoms and molecules adsorbed on their surface provide the possibility of designing sensors on the basis of nanotubes. Several types of gas sensors (detectors) on the basis of the MWCNT are listed here: (1) *Sorption gas sensors*, (2) *Ionization gas sensors*, (3) *Capacitance gas sensors and* (4) *Resonance frequency shift gas sensors* [16].

2 Materials and Methods

2.1 Materials

(a) **PVDF**. PVDF427152-BULK used in this experiment is provided by sigma-Aldrich (Bangalore, India) in pellets form. The material characteristics as provided by the supplier are: the number average M_n is 71×10^3 and weight average is 180×10^3 by GPC, respectively; transition temperature (brittleness temp. −62 °C ASTM D 746 and T_m 155–165 °C; hardness (76–80 shore D, ASTM D 2240); solubility (some polar solvents such as organic esters and amines: soluble).

(b) **MWCNT**. MWCNT 704113-250MG (89% carbon basis; MP: 3652–3697 °C (lit), $\geq$ 99% carbon nanotubes), 0.7–1.3 nm diameter as details provided by the supplier Sigma-Aldrich (Bangalore, India) is considered.

(c) **DMSO**. DMSO 472301-500ML(dimethyl sulfoxide) ACS reagent 99.9% having the characteristics; BP (189 °C), MP (16–19 °C), formula weight: 78.13 g/mol, molecular weight M_w: 78.13 $(CH_3)_2SO$ as detailed by the supplier Sigma-Aldrich (Bangalore, India).

(d) **SDS**. SDS 862010 (sodium dodecyl sulfate); molecular weight M_w: 288.38 $CH_3(CH_2)_{11}OSO_3Na$, $\geq$ 98.5% (GCP): assay 98%, melting point m_p: 204–207 °C(lit), flash point: 170 °C are the characteristics detailed by the supplier Sigma-Aldrich (Bangalore, India).

(e) **Acetone**. acetone (Product ID: 32201-1L) ACS reagent, $\geq$ 99.5% (by GCP). It is also used for identification of ester groups in lipids by spectrophotometric methods having the characteristics; BP: 56 °C/760 mmHg (lit), MP: −94 °C (lit) and flash point: −17 °C as given by the supplier Sigma-Aldrich (Bengaluru, India).

2.2 Solution Preparation

The materials obtained for the experimental study are PVDF, MWCNT and DMSO. The piezoelectricity characteristic of the PVDF material has been used in sensor manufacturing. The master batches of the PVDF and CNT have been mixed with solvent and melted. This molten solution has been used for preparing composite fibers. According to the procedure in Fig. 1, in a beaker placed on the magnetic stirrer PVDF pellets of mass mentioned in Table 1 were added to the beaker. PVDF is insoluble in water. Solvents which are SDS in nature have to be selected for to dissolve them. In this sensor preparation method, DMSO is taken as a solvent for PVDF. After the addition of PVDF pellets into the beaker, the DMSO solvent of ML mentioned in Table 1 is added to the beaker and the magnetic stirrer is set at temp 70 °C. Let the pellets to dissolve in the solvent for at least 3 h, the DMSO itself cannot dissolve completely the PVDF, so we are adding one more SDS to quick the reaction as additive. After the PVDF pellets are dissolved in acetone $(CH_3)_2CO$, the multiwalled carbon nanotubes here considered are in black powder format. It should be added as batch-wise of mentioned MG in Table 1 for better results. Give some gap between each batch for correct rate of mixture. After completing the addition of MWCNT to the solution, add the remaining PVDF pellets for easy dissolvation. The whole solution preparation needs nearly 8 h of time and strict attention for the preparation process. SDS is used as anionic surfactant and for resisting the molecular bonding among PVDF and MWCNT.

2.3 Sensor Preparation

To spun the fiber mat, the electrospun technique was used which converts the polymer solution into fine threads of required diameters such as (hundreds of nanometers ($\sim$250 nm)—hundreds of micrometers ($\sim$250 μm)) which uses strong voltage of electricity (nearly in tens of kV) to deposit the threads on the target (mold). In the melt electrospinning technique, the solution is fed in the solution depositor. The spinneret is attached to cathode (+) of 25 kV, and the target mold is connected to anode (−) at other end. It is considered as most difficult and highly precise method for fiber fabrication which uses the combined properties of both

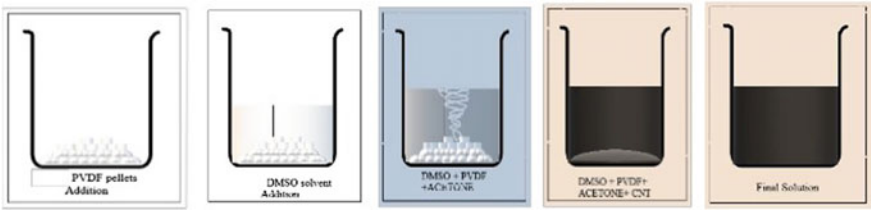

Fig. 1 Sensor solution preparation by the batch-wise addition of composite materials

Table 1 Material quantity details of the samples

Sample	MWCNT (GMS)	PVDF (GMS)	DMSO (GMS)	SDS (GMS)	ACETONE (GMS)
1.	0	0.8	2.5	0.3	2.5
2.	0.2	0.6	2.5	0.3	2.5
3.	0.4	0.4	2.5	0.3	2.5

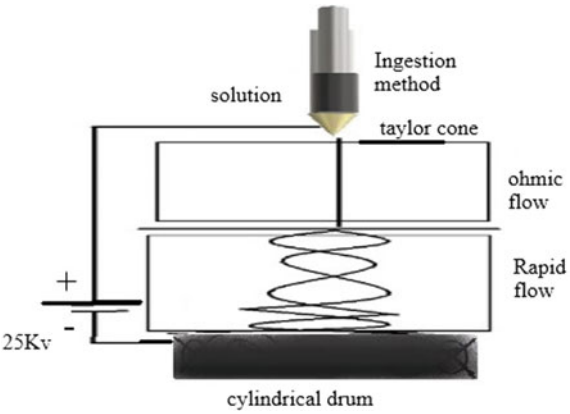

Fig. 2 Sensor preparation on rotating cylindrical drum by ES method

electrospraying and conventional dry spinning of fibers. Due to whipping instability at the initial stage, the fiber is stretched and absent for the process because of low melt conductivity and high viscosity of the melt to overcome this condition 0.05 ml/h feed rate were adopted (Fig. 2).

2.4 Embedding Sensor

The following steps were involved for fabricating the composites plates which embedded with PVDF-MWCNT fiber mat. The 10 layered glass fiber laminates were cut in the dimensions of 300 × 300 mm which is oriented at 0°/90°. By using vacuum infusion resin transfer molding (VARTM) technique, the laminate was manufactured. The resin and hardener used for this study are epoxy resin LY556/ Hardener HY951, respectively. The sensor fiber mat was orientated at 0° to its axial direction, and its performance was monitored during the mechanical test of the nanofiber sensors mat which was placed between 9th and 10th layered sheets by using silver paste. The dimensions of the sensors will be 50 × 2 mm, and it is placed in the center position between the sheets. Now, cover the sheets with a mesh cover to avoid the leakage of resign and cover this with vacuum bag and seal all the portion of the structure. Now, small tubes are inserted into the vacuum bag and some are coming out of it and connected to pressure gauge and vacuum pump. Now, vacuum infusion takes place, the resin and hardener are taken in the

100:12 ratio and allowed to flow in vacuum bag at 25 mm/Hg pressure and at room temperature. After the resin flow over all part of sheet, the process will be stopped. It will be dried for 24 h and after that remove the vacuum bag and mesh cover and take the GFRP laminate from the mold [17].

3 Experimental Procedure

3.1 Characterization of PVDF-MWCNT Fiber

To study the surface morphology and size of electrospun fibers, a scanning electron microscope (SEM) was used. Crystalline phase present in the fiber mats was identified by XRD (X-ray diffraction).

3.2 Incremental Loading and Unloading Tensile Test

Tensile test is done on the samples to find the maximum flexural stress. After finding the maximum flexural stress, the mechanical behavior and matrix composition of the specimen are observed at 25, 35, 45% and also its related stress at that condition. This testing is done as prescribed by the ADTM D3039 standards for tensile properties of polymer matrix composite materials which shows the specimen dimensions as (250 × 25 × 3 mm) is also provided the aluminum tabs to hold by the UTM grips and pulled up to failure observed. Universal testing machine (UTM M-100) considered here has the maximum capacity of 100 kN. The graph of force and displacement is plotted according to the nominal strain (MPa) and nominal stress (%). The curve does not increase constantly because of matrix composite properties. Incremental loading and unloading give the graph which is shown as retrograde.

3.3 Three-Point Bending Test

Three-point bending test is used to find the flexural properties from bending displacement of the samples. The maximum flexural stress is found by the bending displacement and also the condition of fiber mat at different percentage of maximum flexural stress. This testing is done according to the ASTM D790 bending test of unreinforced and reinforced plastics and an electrical insulating material which shows the specimen dimensions as (150 × 25 × 3 mm) placed on the two knife edges at equal distance from the tip. The load is applied at the center of the fiber mat in incremental and decremental loading condition. The graph is plotted as flexural stress (MPa) versus flexural strain (%). The maximum flexural stress of the fiber

mat is also finding out in this bending method. Due to this, the maximum flexural stress at 25, 30, 45% and also the failure in the fiber mat are observed at particular percentage of the load.

4 Result and Discussion

4.1 Morphological and Phase Behavior Analysis

From SEM image, homogeneously dispersed MWCNT was observed in PVDF matrix. SEM image of PVDF fiber mat and PVDF-MWCNT fiber mat is shown in Fig. 3.

And in order to determine the reinforcement effect, such as mechanical behaviors, crystallization and piezoelectricity of MWCNT in aligned PVDF fibers, interfacial adhesion between MWCNT and PVDF chains are two major factors. The crystalline structure of PVDF/MWCNT fiber mat is characterized by XRD spectrum. The diffraction peak at $2\theta = 21°$ is observed, which generally represents the β-crystalline PVDF formation, as shown in Fig. 4.

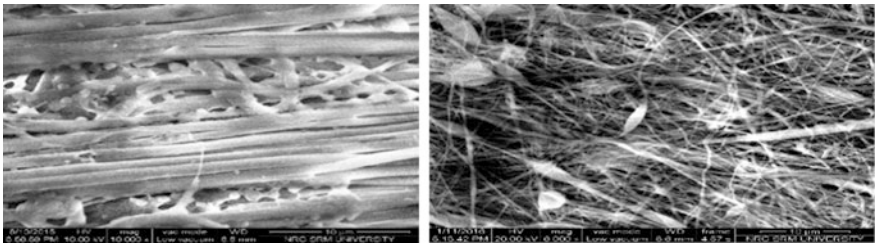

Fig. 3 SEM images of PVDF fiber mat and PVDF-MWCNT fiber mat

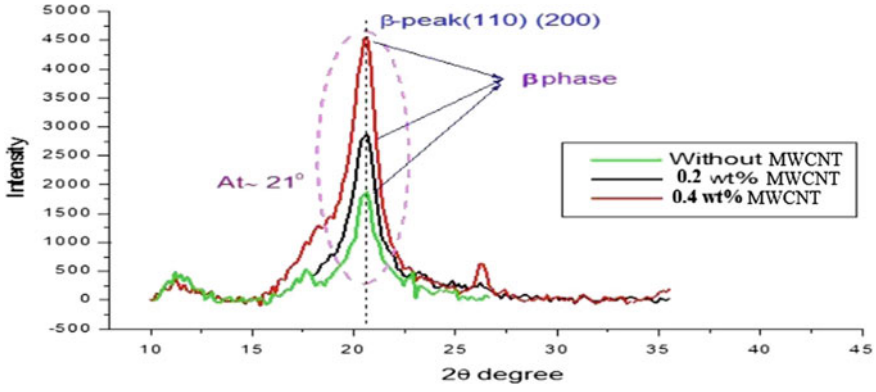

Fig. 4 XRD diffraction of PVDF-MWCNT fiber

4.2 Tensile Test

The tensile test has been conducted for three types of samples in which, one set of sample was embedded such as 0, 0.2 and 0.4 wt% of MWCNT. Initially, the tensile testing was conducted on the specimen untill it fractures. From that, the fracture stress was found out, and the four incremental loading–unloading procedures were done for all the specimen according to the fracture stress obtained in order of 20, 35, 45 and 100%. Figure 5 represents the typical mechanical response of different MWCNT wt%.

For the initial tensile test, glass fiber without MWCNT specimen has been taken and the first mechanical load of 120 MPa stress has been applied on the specimen, which shows the increase in strain according to the load (stress) applied. Then, the second mechanical load of 310 MPa and third mechanical load of 493 MPa stress show the gradual level of increase according to the stress fracture which can be seen in graph, and the curve does not follow the same growth which shows the matrix crack or debonding that occurs in fiber. During fourth mechanical load of 613 MPa on the specimen, further increase in the load tends to be fiber damage or material damage. In the graph, it is shown that GFRP without MWCNT withstands the stress level of (445MPa) and GFRP with MWCNT of 0.2 wt% withstands (535MPa) and GFRP with MWCNT of 0.4 wt% withstands (650 MPa), and show that the increase in MWCNT concentration increases the strength of the material. In aerospace designing, mechanical stress has been widely preferred due to its mechanical property. During mechanical load, its resistance has been monitored and shows the electrical resistance reading of MWCNT fiber which is proportional to the applied stress. Thus, MWCNT has an essential attribute in calculating the inherent damage in composite material by performing simple tension test.

4.3 Three-Point Bending Moment Result

PVDF-MWCNT sensor in tension region

The ability of the embedded sensor which is PVDF-MWCNT fiber mat to sense the damage on the composite structures during loading conditions was analyzed by using the three-point bending test. The damages such as matrix crack, fiber breakage and debending can be detected by measuring the change in electrical resistance which can be related to the residual strain stored in the material during different loading condition which could result in damage. In the present study, the plot was drawn between the change in electrical resistance versus nominal strain of the FRP specimen embedded with PVDF-MWCNT fiber mat. Figure 6 shows that the ratio of $\Delta R/R_0$ and nominal strain for the different wt% of MWCNT such as 0, 0.2 and 0.4wt%. When the nominal strain increases the corresponding change in electrical resistance increases for all the wt% of MWCNT else 0 wt% does not change in path toward change in electrical resistance. It is clearly understood that the 0 wt% of MWCNT fiber mat embedded between the GFRP has no variation in resistance increasing the value of nominal strain.

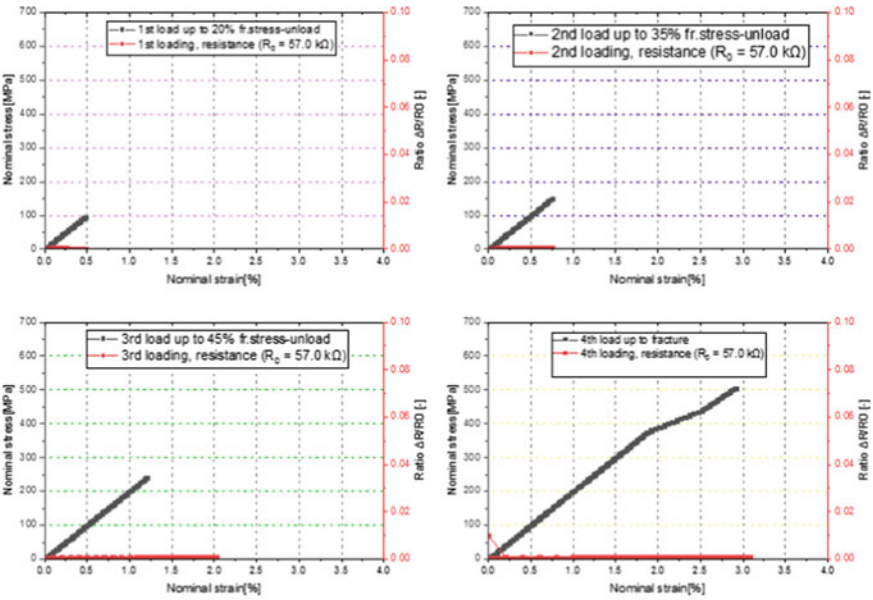

(a) 0 wt.% MWCNT

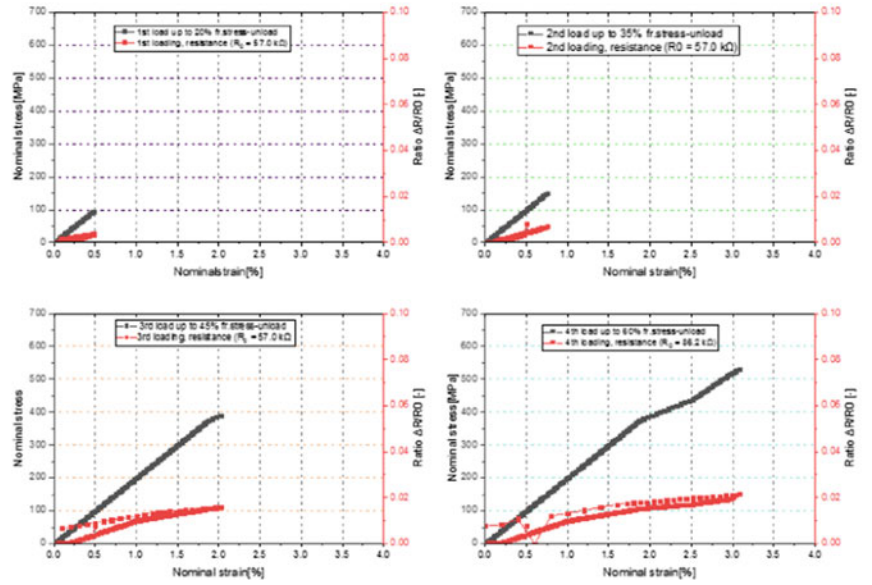

(b) 0.2 wt.% MWCNT

Fig. 5 Typical tensile mechanical and resistance results of GFRP specimen with embedded PVDF-MWCNT with electrical resistance change of **a** 0 wt% MWCNT, **b** 0.2 wt% MWCNT, **c** 0.4 wt% MWCNT

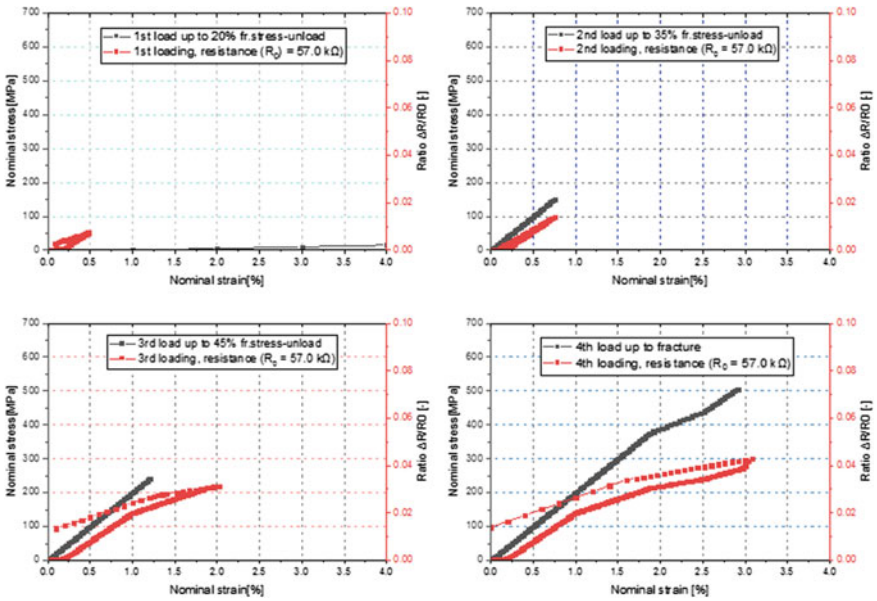

(c) 0.4 wt.% MWCNT

Fig. 5 (continued)

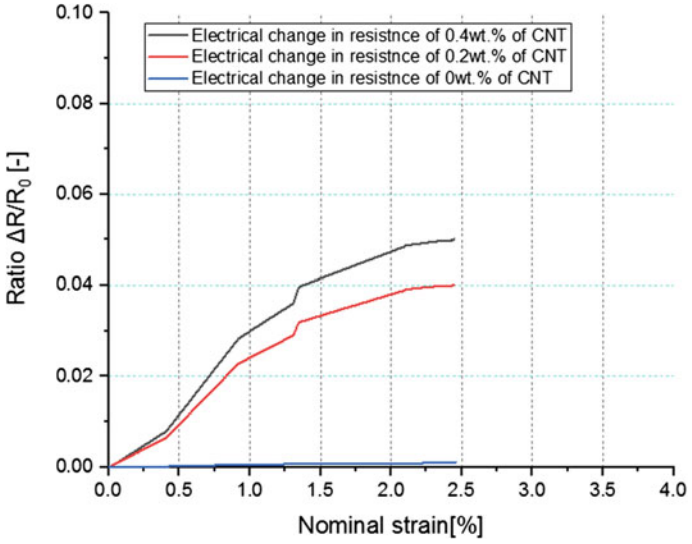

Fig. 6 Typical electrical resistance result of different MWCNT wt% in nominal strain region

5 Conclusion

The glass fiber reinforced polymer (GFRP) samples embedded with PVDF-MWCNT fiber mat has manufactured in order to determine the damages on the aircraft structure through its electrical resistance measurement. In the present study, the following conclusions were obtained: MWCNT has electrical conductive property when PVDF-MWCNT fiber mat embedded between the nonconductive GFRP laminate. The GFRP specimen becomes conductive in order to measure the change in resistance through silver paste and conductive cables. The dispersion of MWCNT and PVDF was analyzed by using SEM technique and its electrical conduct property was analyzed by XRD. Electrospinner technique was adopted to obtain the ultra-thin fiber mat sensor which will not degrade the mechanical property of manufactured specimen. The VARTM process was adopted in order to obtain the smoothly finished sample. Two types of mechanical test were carried out such as tensile test and three-point bending test. In both the test, it has proved that when the mechanical loading was applied its corresponding change in electrical resistance was monitored. When the change in electrical resistance varies abnormally the specimen leads to damage in the structure.

References

1. Composite materials. Royal Society of Chemistry/Advancing the chemical science. www.rsc.org/Education/Teachers/Resources/Inspirational/Resources/4.3.1.pdf
2. Composites in aerospace applications by Adam Quilter on Oct 1, 2004. www.avaitionpros.com/article/1038644/compOsites
3. Deo, R.B., Starner, J.H., Holzwarth, R.C.: Low-cost composite materials and structures for aircraft applications, May 2001
4. Witten, E., Kraustkuhnel, M.: Composites market report 2017. http://www.euciaeu/userfiles/composites-Market%20report-2015pdf.
5. Determination of fracture causes in an aircraft motor cylinders. Eng. Fail. Anal. **82**, 812–822 (2017)
6. Hu, H., Belouettar, S., Potier-Ferry, M., Makradi, A., A novel, finite element for global and local buckling analysis of sandwich beams. Comp. Struct. **90,** 270–278 (2009)
7. Katunin, A., Dragon, K., Dziendzikowski, M.: Damage identification in aircraft composite structures: a case study using a various non-destructive testing techniques. Comp. Struct. **127**, 1–9 (2015)
8. Soyoz, S., Feng, M.Q.: Instantaneous damage detection of bridge structure and experimental verification. Struct. Control Health Monit. **15**(7), 958–973 (2008)
9. Boller, C., Chang, F.-K., Fujino, Y.: Encyclopedia of structural health monitoring. Wiley, New York (2009)
10. Balageas, D., Fritzen, C., Guemes, A. (eds.): Structural health monitoring. ISTE, London, Newport Beach, CA (2006)
11. Giurgiutiu, V.: Structural health monitoring with piezoelectric wafer active sensors. Elsevier, Oxford (2008)
12. Garg, D.P., Zikry, M.A., Anderson, G.L., Stepp, D.: Struct Health Monit **1**, 23–39 (2002)

13. Farrar, C.R., wooden, K.: Structural health monitoring: a machine warning prospective. Willey, Chichester, UK (2013)
14. Friswell, M.I., Adhikari, S.: Structural health monitoring using shape sensors, Mech. Syst. Signal Process. **24**, 623–635 (2010)
15. Focus on landing gear via SHM & sensors. In: 6th European workshop on SHM, detect tolerant, safe life
16. Zaporotskova, I.V., Boroznina, N.P., Parkhomenko, Y.N., Kozhihor, L.V.: Carbon nanotubes: sensor properties. A review. Mod. Electron. Mater. **2**, 95–105 (2016). National University of Science and Technology Misis, 10th Jan 2017
17. Nisha, M.S., Singh, D.: Manufacturing of smart nanomaterials for structural health monitoring (SHM) in aerospace application using CNT and CNF. J. Nano Res. **37**, 42–50 (2016)